CrossMark

ORIGINAL PAPER

In vitro and in vivo evaluation of the toxicities induced by metallic nickel nano and fine particles

Ruth Magaye[1] · Yuanliang Gu[1] · Yafei Wang[1] · Hong Su[1] · Qi Zhou[1] ·
Guochuan Mao[1] · Hongbo Shi[1] · Xia Yue[1] · Baobo Zou[1] · Jin Xu[1] ·
Jinshun Zhao[1] (ORCID)

Abstract Nickel nanoparticles (Ni NPs) have been applied in various fields along with the rapid development of nanotechnology. However, the potential adverse health effects of the Ni NPs are unclear. To investigate the cyto- and genotoxicity and compare the differences between the Ni NPs and the nickel fine particles (Ni FPs), Sprague-Dawley (SD) rats and A549 cells were treated with different doses of Ni NPs or FPs. Intra-tracheal instillation of Ni NPs and FPs caused acute toxicity in the lungs, liver and kidneys of the SD rats. Even though the histology of the lungs showed hyperplastic changes and the protein expression of HO-1 and Nrf2 detected by western blot showed lung burden overload, no significant increase was observed to the expression level of oncoprotein C-myc. The results from cell titer-Glo assay and comet assay indicated that Ni NPs were more potent in causing cell toxicity and genotoxicity in vitro than Ni FPs. In addition, Ni NPs increased the expression of C-myc in vitro, but these increases may not have been due to oxidative stress since no significant dose-dependent changes were seen in HO-1 and Nrf2 expressions. Although Ni NPs have the potential to cause DNA damage in A549 cells in vitro, the molecular mechanisms that led to these changes and their tumorigenic potential is still debatable. In short, Ni NPs were more potent in causing cell toxicity and genotoxicity in vitro than Ni FPs, and intra-tracheal instillation of Ni NPs and FPs caused toxicity in organs of the SD rats, while it showed similar to the effects for both particle types. These results suggested that both Ni NPs and FPs have the potential to be harmful to human health, and Ni NPs may have higher cyto- and genotoxic effects than Ni FPs under the same treatment dose.

Abbreviations

Ni FPs	Nickel fine particles
Ni NPs	Nickel nanoparticles
SD rat	Sprague dawley rat
IARC	International Agency for Research in Cancer
SEM	Scanning electron microscopy
TP	Total protein
ALP	Alkaline phosphatase
AST	Aspartate transaminase
ALT	Alanine aminotransferase
Total B	Total bilirubin
Direct B	Conjugated bilirubin
BUN	Blood urea nitrogen
CK	Creatine kinase
CK-MB	Creatine kinase isoenzymes
HDL-C	High-density lipoproteincholesterol
WBC	Whole blood count
NE%	Neutrophil %
Ly%	Lymphocyte %
Mo%	Monocyte %
Eo%	Eosinophil %
RBC	Red blood cells
HGB	Hemoglobin
MCHC	Mean corpuscular hemoglobin concentration

Ruth Magaye, Yuanliang Gu and Yafei Wang contributed equally to this work.

✉ Jinshun Zhao
zhaojinshun@nbu.edu.cn

[1] Department of Preventative Medicine, Zhejiang Provincial Key Laboratory of Pathological and Physiological Technology, Medicine School of Ningbo University, 818 Fenghua Road, Jiangbei District, Ningbo 315211, China

PLT   Platelet
CKD   Chronic kidney disease
CAD   Coronary artery disease

Background

The respiratory system is the most common route of exposure to particulate matter. The increased production and use of nanomaterials, poses a risk for respiratory disorders (Elbastawisy and Almasry 2014). This has led to the need for epidemiological and toxicological research data in regards to the effects of the nanoparticle (NP) materials, size range of <1 to <100 nm in diameter, (Morimoto et al. 2010; Mueller et al. 2012) such as nickel (Ni). There is evidence of Ni compounds in their bulk or fine states having toxic and genotoxic effects on the respiratory system (Ke et al. 2008; Lu et al. 2005). The International Agency for Research in Cancer (IARC) have also classed it as a carcinogen. This has warranted a lot of research into the different types of NPs and their toxicity and genotoxicity mechanisms.

Most in vivo studies on Ni NPs have been focused on pulmonary pathology, whether by intra-tracheal instillation (Ada et al. 2010; Baek and An 2011; Das and Buchner 2007) or whole body inhalation systems (Ogami et al. 2009; Oyabu et al. 2007). Ni NP compounds such as Ni hydroxide and NiO have been shown to induce inflammatory effects in the lungs in both long and short term studies of intra-tracheal instillation and whole body inhalation exposure, respectively (Ahamed 2011; Baek and An 2011; Gillespie et al. 2010). Intramuscular implants of Ni NPs were shown to induce rhabdomyosarcomas in rats by Hansen et al. (2006). We have previously shown that Ni NPs (50 nm) can cause liver and spleen injury, lung inflammation and cardiac toxicity when injected intravenously to the SD rats (Magaye et al. 2014). Epidemiological studies regarding the carcinogenesis of the metallic Ni NPs are currently lacking (Magaye and Zhao 2012).

In vitro studies have also demonstrated that NP compounds and NPs can cause cyto- and genotoxicity through factors such as oxidative stress that lead to deregulation of apoptosis pathways, (Ahamed 2011; Ahamed et al. 2011; Ahamed and Alhadlaq 2014; Park et al. 2007; Shi et al. 2013) inflammation, (Baek and An 2011; Gillespie et al. 2010) and DNA damage (Alarifi et al. 2014; Huk et al. 2015; Zhao et al. 2009b). However, research on the carcinogenicity of metallic Ni NPs is still insufficient (Sivulka 2005). In the previous study, we found that the genotoxic effects of NPs demonstrated ranged from DNA damage and upregulation and activation of genes such as AIF, Akt and

Bcl-2 in JB6 cells (Zhao et al. 2009a). Deregulation of the apoptosis pathway can form the basis for numerous pathological processes including induction of neoplasm development (Zaman et al. 2015; Zou et al. 2016). A lot of factors can cause apoptosis to occur, apart from the normal physiological response, disruptions to any one of the enzymes and proteins in its pathway can have detrimental effects. Deregulation of the apoptosis pathway can be caused by oxidative stress due to reactive oxygen species (ROS) (Liu et al. 2016; Yang et al. 2016). Studies have shown that oxidative stress may be a key route in inducing the cytotoxicity of NPs (Ahmad et al. 2016; Fahmy and Cormier 2009; Pujalte et al. 2011; Yang et al. 2009). Ahamed et al. (2011) showed that Ni NPs induced ROS in dose and time dependent manner in A549 cells treated with 0, 1, 2, 5, 10 and 25 µg/mL for 24–48 h. Another study on A549 cells found that NiO (20 nm) increased the gene expression of Hemeoxygenase-1 (HO-1), (Horie et al. 2011) a stress-responsive enzyme that acts during inflammatory reactions (Neubauer et al. 2015). Oxidative stress also poses a big threat because it can lead to mitochondria dysfunction, DNA, protein and lipid damage (Dorighello et al. 2016; Ryter et al. 2007).

Here we have used both in vitro and in vivo studies to determine the cyto- and genotoxicity of the metallic Ni NPs and FPs. As a means to focus our study on the pulmonary system, our study used intra-tracheal instillation method for in vivo and A549 cells (a human lung alveolar epithelial adenocarcinoma cell line) for in vitro experiments.

Materials and methods

Particle preparation

A stock suspension of Ni NPs and FPs was prepared in normal saline (10 mg/mL) by sonication for 30 s using a Branson sonifier 450 (Branson Ultrasonics Corp., Danbury, CT) for the in vivo experiment. The particle suspensions were kept on ice for 15 s and sonicated again on ice for a total of 3 min at a power of 400 W. Before use, Ni NPs and FPs were diluted to desired concentrations in fresh saline. The same preparation method was used to prepare Ni NPs and FPs in PBS (phosphate buffered solution) for the in vitro experiments. From this stock solution, aliquots of desired concentrations were then added to the cell culture or intra-tracheally instilled to rats. All samples were prepared under sterile conditions.

Detection of particle size distribution

The size distribution of the Ni NPs and FPs were determined using SEM. Ni NPs and FPs were prepared by sonication.

The surface area of the particles was measured using the Gemini 2360 Surface Area Analyzer, with a flowing gas technique according to the manufacturer's instructions. Then, the samples were diluted in double-distilled water and air dried onto a carbon planchet. Images were collected on a SEM, according to the manufacturer's instructions. Optimas 6.5 image analysis software was used to measure the diameter of the particles. About the hydrated particle size of Ni NPs, it was checked in our early published study, certain agglomerates of Ni NPs in the solution could be found under the microscope (Magaye et al. 2014).

In vitro studies

Cell viability test

Following the manufacturer's instructions for the cell titer-Glo assay (Promega, USA), 1×10^5 A549 cells/well were seeded in a 96 well plate and incubated overnight at 37 °C and 5 % CO_2 in 100μL 10 % FBS/DMEM. The cells were then treated with varying dose ranges of Ni NPs or FPs (0, 1, 5, 10, 15 and 25 μg/cm^2) in replicates of three. These were then incubated overnight. Following the manufacturer's instructions, the ATP concentration was detected using the cell titer-Glo assay. The results were accepted if the R^2 for the standard curve was ≥0.95.

Lung tissue protein extraction

Lung tissue samples weighing approximately 10–30 mg were flash frozen in liquid nitrogen. These were then stored at −80 °C until used. The lung tissues were then grounded with a motar and pestel in liquid nitrogen. 100 μL of lysis containing 10 mmol/L PMSF and 1 mM EDTA were then added to the tissue residue. This was then aspirated and placed in 1.5 mL eppendoff tubes. The solution was left for 1 h on the shaker in ice to fully lyse the tissue residue. After lysis, the cells were then centrifuged at 15,000 rpm for 5 min at 4 °C. The supernatant was then transferred into another eppendoff tube and the protein concentration was determined using BCA assay. These were then stored at −20 °C until use.

Western blot

A549 cells were incubated with and without Ni NPs or FPs in 25 cm^2 culture flasks for 24 h. The cells were then lysed with 200 μL of lysis containing 10 mmol/L PMSF and 1 mM EDTA on ice. Rubber policemen were used to gently scrape the cells. The residual solution with cells were aspirated and transferred into 1.5 mL eppendoff tubes. The cells were then centrifuged at 15,000 rpm for 5 min at 4 °C. The supernatant was collected and protein concentration determined using BCA assay. The samples were stored at −20 °C until use.

The A549 cell and rat lung protein concentrates (50 μg) were denatured for 5 min at 95 °C, electrophoresed through 10 % SDS PAGE, and transferred onto PVDF membranes (Saradhi et al. 2005). After proteins were transferred, they were stained with Ponceau S to confirm protein transfer. The blots were then blocked in 5 % milk blocking buffer for 3 h and incubated overnight at 4 °C with the primary antibody of interest. HO-1 or C-myc antibody were respectively diluted in 5 % milk blocking buffer (Cell signaling Technologies) at 1:1000 and β-actin antibody (Beyotime) at 1:10,000. The blots were washed with TBST, before addition of the IgH HRP secondary antibody at 1:1000 and incubation at room temperature for 2 h. The blots were then washed with TBST, and the fluorescence detected. The images were captured and developed using Bio-Rad's image capture system (Bio-Rad, USA) and the quantity one software was used for band analysis.

Comet assay

1×10^5 A549 cells cultured in 6 well plates were treated with and without Ni NPs and FPs and incubated for 24 h. The cells were then detached with 1 mL of 0.25 % trypsin. 1×10^5 cells in PBS suspension were aliquoted into 1.5 mL eppendoff tubes. For the positive control group, 100 μM H_2O_2 was added and placed at 4 °C for 20 min. The comet assay was done according to the manufacturer's instructions (Trevigen's, USA). Briefly, The LM agarose gel was pre-boiled for 5 min at 90–100 °C. It was then cooled in 37 °C water bath for 20 min. Then, 5 μL of the 1×10^5 cell suspension was added to 50 μL of LM agarose in an eppendoff tube. 50 μL of this mixture was placed onto the comet slide, and spread evenly and placed at 4 °C in the dark for 30 min to gel. The slides were then immersed in pre-chilled lysis solution at 4 °C for 1 h. These were then immersed in freshly prepared alkaline unwinding solution (pH > 13) at room temperature in the dark for 1 h. The slides were then removed and placed in the horizontal electrophoresis tank (Beijing, China), containing alkaline electrophoresis solution and run at 24 V and 300 Am for 30 min. The slides were then rinsed in two changes of double-distilled water for 5 min each and fixed in 1 change of 70 % ethanol for 5 min. These were then dried at ≤45 °C for 15 min. Then 100 μL of diluted SYBR green was added onto each well of agarose gel and placed at 4 °C for 5 min. After removing excess SYBR green and dried completely at room temperature in the dark, the DNA damage caused by Ni NPs and FPs in A549 cells were analyzed by examining the cells under the Olympus inverted microscope and quantified by scoring comets as a result of DNA damage. 40 cells were counted in 3 different

experiments. The comets were scored using Comet Score software from Trek technology.

In vivo studies

Study design

Healthy SD rats (6 weeks old) were selected and randomly divided into 3 treatment groups (5.6, 12 and 25 mg/kg) with 5 male animals in each group for each particle type. A total of 7 study groups including the control were used. Dose ranges selection was based on Zhang et al. (2003) study. The Horn's method was used to calculate the 2 lower dose levels from the highest dose level (25 mg/kg).

Animal husbandry

All animals (35 rats) were housed according to standard animal housing conditions (relative humidity at 60 ± 10 %, room temperature of 20 ± 2 °C and a 12 h light/dark cycle). The SD rats were fed standard laboratory chow. Food and water were provided ad libitum. All animals were kept in stress free, hygienic and animal-friendly conditions. Animal study protocols were approved by the Ningbo University Institutional Animal Care and Use Committee.

Dose preparation

The average body weight of the SD rats was to be 0.16 kg. Using this average weight, 1 mL stock solutions of Ni NPs or FPs (18, 39 and 83.5 mg/mL) suspended in normal saline was sonicated for 5 min and vortexed before use.

Intra-tracheal instillation

The SD rats were anesthesized with ether (5 %) prior to intra-tracheal instillation of Ni NPs or FPs. While the rat was under anesthesia, it was secured by its incisors to a stand using a string at a 90 degree angel. A catheter was then inserted transorally into the tracheal lumen which was exposed by gently pulling the tongue to one side. Each SD rat was intra-tracheally instilled through the catheter with 0.05 mL of either Ni NPs or FPs. The control group received normal saline in the same manner. The SD rats were then placed in clean housing with heated lamp for recovery. The rats were sacrificed at day 14 after instillation.

Hematological analysis of blood parameters

Evaluation of hematological parameters was done at Ningbo No. 3 hospital (Ningbo, China). After the animal was anesthetized, 5 mL blood for hematological analysis was collected into a test tube by incision of the femoral

artery. All animals were sacrificed at the same time. Of this sample 1 mL was collected into the test tube containing 20 mg/mL EDTA anticoagulant for complete blood count (CBC) and the remaining 4 mL for biochemical analysis. The blood was analyzed for the number of erythrocytes, platelets, total white blood cells (WBC) as well as WBC differentials by an automated blood analyzer (sysmex XT-1800i, Japan). Apart from these other parameters such as hemoglobin (HGB) and MCHC were also analyzed.

Biochemical analysis of blood serum parameters

Enzymatic parameters related to liver, kidneys and cardiac function were analyzed. Analysis of lipid and serum electrolytes, were also included. All biochemical analysis was done at Ningbo No. 3 hospital (Ningbo, China). The Hitachi 7600-110 auto analyzer (Hitachi, Tokyo, Japan) was used.

Histopathological examination

The formalin fixed tissues were stored at 4 °C until examination. Tissues were processed using standard histology laboratory techniques. Using a microtome, 3–4 mm sections were cut. These were then stained with hematoxylin and eosin stain using standard staining protocols.

Statistical analysis

Statistical analysis was performed with a 2-sample t test, unknown and unequal variances, comparing each sample group to the related control group and ANOVA was used for multiple group comparisons. P values ≤ 0.05 were accepted as significant. The results are presented as mean ± standard deviation (SD).

Result

Particle size distribution

Figure 1 shows the images of the FPs (A) and NPs (B) used in this study detected by SEM. The data from Table 1 show that the size of Ni NPs was 40.50 ± 18.6 nm, and the mean surface area was 28 m^2/g; the size of Ni FPs was 350 ± 87 nm, and the mean surface area was 0.37 m^2/g.

In vitro studies

Cell viability

Figure 2 shows the comparative cytotoxicity of Ni NPs and Ni FPs. A significant decrease in cell viability at 5, 10, 15 and 25 μg/cm^2 dose ranges were observed for both Ni NPs

Fig. 1 SEM images of the particles used in this study. *Notes* **a** Ni FPs; **b** Ni NPs. *SEM* scanning electron microscopy, *Ni FPs* nickel fine particles, *Ni NPs* nickel nanoparticles
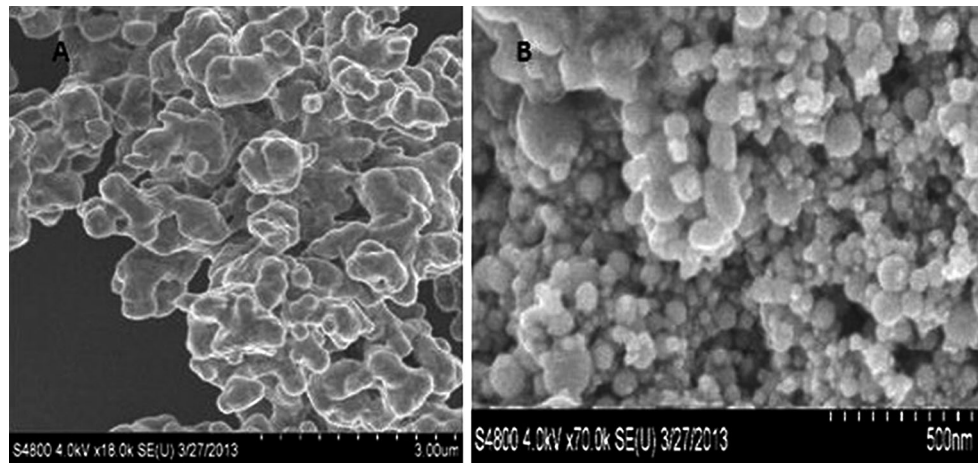

Table 1 Physicochemical characteristic of Ni NPs and FPs

Sample	Primary size measured by		Surface area (mean $\pm$ SD) (m^2/g)	Composition
	Manufacturer (nm)	SEM (mean $\pm$ SD) (nm)		
Ni NPs	50	40.50 ± 18.6	28 ± 0.02	99.8 % Ni 0.01 % Co 0.0068 % Ca
Ni FPs	>100	350 ± 87	0.37 ± 0.01	99.9 % Ni

SEM scanning electron microscopy, *Ni NPs* nickel nanoparticles, *Ni FPs* nickel fine particles
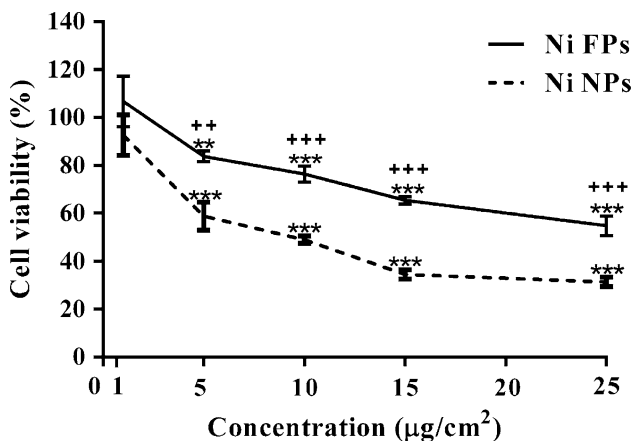

Fig. 2 Comparative cytotoxicity of Ni NPs and FPs. *Notes* cell viability was determined by measuring the ATP concentration. Cell viability rate was normalized to that of the control. *Bars* represented (mean $\pm$ SD) values of 3 experiments. *Ni FPs* nickel fine particles, *Ni NPs* nickel nanoparticles

and FPs treated groups when compared to the control. In addition, the decrease in cell viability for the Ni NPs treated groups was greater than Ni FPs treated groups.

Western blot analysis

The western blot analysis of the HO-1 protein expression of A549 cells treated with Ni NPs or FPs showed a significant increase in all dose groups of both particle types (Fig. 3a)

compared to the control. When compared to Ni FPs treated group, the increase of HO-1 expression of Ni NPs treated group was greater in the 1 and 15 μg/cm^2 dose groups, and vise versa for the 10 and 25 μg/cm^2 dose groups. A significant increase in the C-myc protein expression was only observed in A549 cells treated with Ni NPs (Fig. 3b) compared to the control. A significant decrease of Nrf2 protein expressions were observed in A549 cells treated with both Ni NPs and FPs at 25 μg/cm^2 (Fig. 3c) compared to the control.

Comet assay

The pictorial images shown in Fig. 4 show that at all dose ranges, the Ni NPs caused some damage to the cells when compared to the control. However, when quantified this damage a significant increase was found at 10, 15 and 25 μg/cm^2 in Ni NPs treatment groups (Fig. 5). While, the DNA damage was only significant increase for the high dose group (25 μg/cm^2) for the cells treated with Ni FPs.

In vivo studies

Biochemical parameters

Biochemical analysis was carried out on the serum of the blood of the SD rats treated with Ni NPs or FPs for biochemical evidence of acute toxicity in vivo (as shown in Table 2).
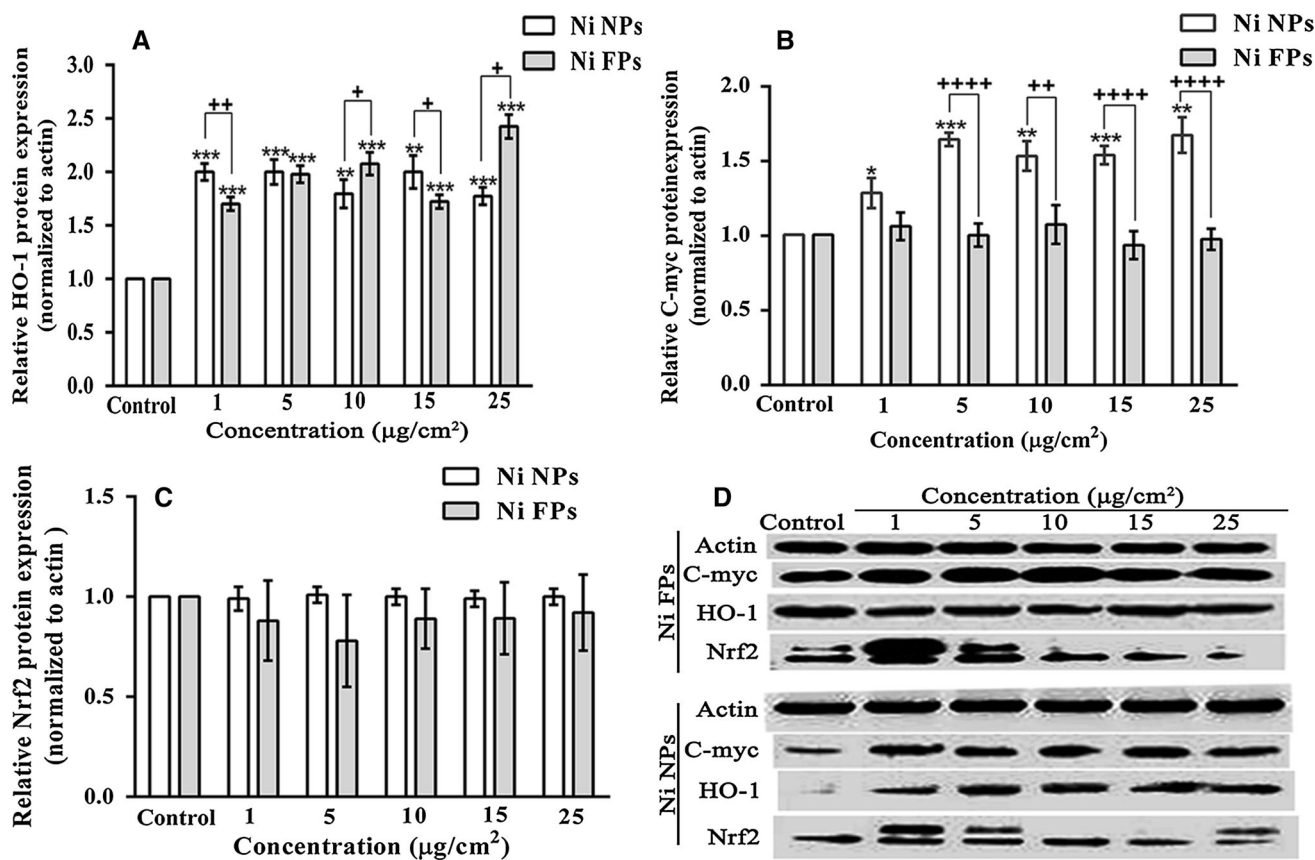
Fig. 3 HO-1, Nrf2 and C-myc protein expressions in A549 cells. *Note* **a** the relative HO-1 protein expression, **b** the relative C-myc protein expression, **c** the relative Nrf2 protein expression, **d** western blot images of HO-1, Nrf2 and C-myc. Relative values were normalized to β-actin. *Bars* represent (mean ± SD) the expressions of each protein in 3 different blots ($*P < 0.05$, $**P < 0.01$, $***P < 0.005$, $****P < 0.001$, vs. control; $^+P < 0.05$, $^{++}P < 0.01$, $^{+++}P < 0.005$, $^{++++}P < 0.001$). *Ni FPs* nickel fine particles, *Ni NPs* nickel nanoparticles

Fig. 4 Images of comet assay in A549 cells. *Notes* cells without any treatment was set as the negative control (C⁻). The positive control was treated with 100 μM H_2O_2(C⁺). *Ni FPs* nickel fine particles, *Ni NPs* nickel nanoparticles
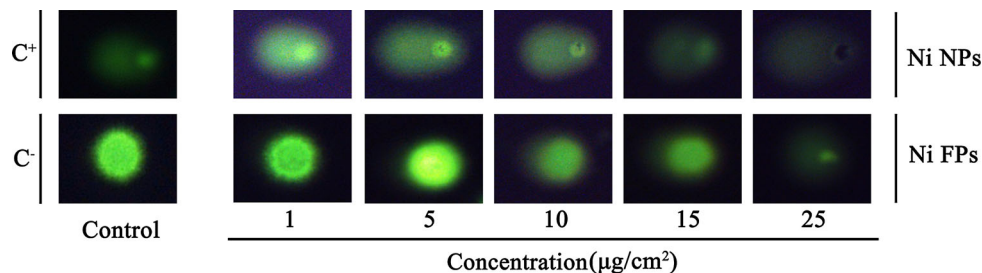
Hematological parameters

Hematological analysis was carried out on the blood of the SD rats treated with Ni NP or FP for hematological evidence of acute toxicity in vivo (as shown in Table 3).

Histopathological examination

In order to determine the pathological effects caused by Ni NPs and FPs, the tissues of the rats were examined. The lung and liver of all dose groups showed prominent and distinguishable pathological changes (as shown in Figs. 6, 7).

Western blot analysis (lung tissues)

Western blot analysis of the expressions of HO-1, Nrf2 and C-myc proteins were carried out on small sections of the lung tissues.

There was a significant decrease in the expression of HO-1 in the lung tissues of Ni NPs treated groups (12 and 25 μg/cm²) and Ni FPs treated group (5.6 μg/cm²) when
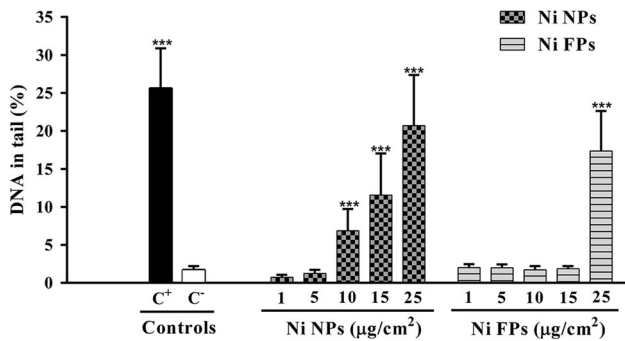
Fig. 5 The percentages of A549 cells with DNA comet tails. *Notes* cells without any treatment was set as the negative control (C^-). The positive control was treated with 100 µM $H_2O_2(C^+)$. *Bars* represent (mean ± SD) percentages of cells with DNA tails in 40 individual comets counted from 2 parallel slides (***$P < 0.001$ vs. control). *Ni FPs* nickel fine particles, *Ni NPs* nickel nanoparticles

compared to the control (Fig. 8a). While, the decrease in HO-1 expression in the lung tissues of Ni FPs treated groups was also significant when compared to Ni NPs treated group. The western blot analysis of the lung tissues showed no significant changes in the C-myc protein expression (Fig. 8b) in both Ni NPs and FPs treated rats. A significant dose–response decrease in the expressions of Nrf2 in the lung tissues in both Ni NPs and Ni FPs treated rats was found when compared to the control (Fig. 8c).

Discussion

The metallic Ni NP is a product with many characteristics including a high level of surface energy, high magnetism, low melting point, high surface area, and low

Table 2 Biochemical parameters of 35 SD rats after treatments with Ni NPs or FPs

Parameters	Control	Ni NPs (mg/kg)			Ni FPs (mg/kg)		
		5.6	12	25	5.6	12	25
Liver profile							
TP (g/L)	49.3 ± 3.4	51.3 ± 1.5	52.4 ± 1.4	51.12 ± 2.1	53.8 ± 1.1*	52.42 ± 0.9	52.86 ± 2.01
Albumin (g/L)	29.3 ± 1.6	30.7 ± 0.8	30.8 ± 1	30.2 ± 1.02	32.1 ± 1*	31.42 ± 0.9*	30.8 ± 0.6
ALP (U/L)	345.8 ± 64.8	427.4 ± 102	379.2 ± 88.8	452 ± 87.9	277 ± 60.7	329.6 ± 45.9	317.8 ± 20.9
AST (U/L)	169 ± 32.8	183.8 ± 37.9	160.6 ± 70.5	148.2 ± 29.6	129 ± 28	134.6 ± 13.8	137.6 ± 15.5
ALT(U/L)	75.6 ± 9.2	78.2 ± 4.6	82 ± 28.5	79 ± 16.7	59 ± 9.4*	63 ± 3.2*	69.4 ± 9.4
Total B (umol/L)	0.88 ± 0.19	0.42 ± 0.26**	0.52 ± 0.1**	0.44 ± 0.17***	0.82 ± 0.31	0.58 ± 0.44	0.36 ± 0.17***
Direct B (umol/L)	1 ± 0.3	0.76 ± 0.21	0.68 ± 0.23*	0.6 ± 0.16**	0.9 ± 0.33	0.96 ± 0.34	0.36 ± 0.2***
Renal profile							
BUN (mmol/L)	6.7 ± 0.8	6.6 ± 0.5	6.7 ± 0.5	6.6 ± 0.4	6.2 ± 1	5.5 ± 0.9*	5.4 ± 0.4**
Creatinine (umol/L)	20.6 ± 2.7	17.6 ± 2.6	18.2 ± 1.6	16.2 ± 2.3*	17.6 ± 2.6	15.0 ± 2.6**	17.8 ± 2.2
Uric Acid (umol/L)	110.8 ± 24.4	114 ± 31.6	95.8 ± 22.3	139.6 ± 41.6	102.2 ± 22.4	103 ± 16.3	130.4 ± 24.2
Cardiac profile							
CK (U/L)	3913 ± 743	6087 ± 747*	1351 ± 378*	1788 ± 555*	1263 ± 206*	1715 ± 386*	1640 ± 602*
CK-MB (U/L)	1024 ± 132	1327 ± 336	750 ± 59*	1236 ± 285	749 ± 66*	875 ± 86	1065 ± 226
Lipid profile							
Cholestrol (mmol/L)	1.8 ± 0.2	1.8 ± 0.2	1.9 ± 0.2	1.8 ± 0.3	1.8 ± 0.4	1.6 ± 0.1	1.9 ± 0.2
Triglycerides (mmol/L)	0.9 ± 0.3	1.3 ± 0.3*	1.2 ± 0.2*	1.2 ± 0.6	0.9 ± 0.3	0.7 ± 0.3	1.5 ± 0.3**
HDL-C (mmol/L)	0.8 ± 0.1	0.8 ± 0.1	0.9 ± 0.1	0.9 ± 0.1	0.71 ± 0.1	0.7 ± 0	0.8 ± 0.1
Serum electrolytes							
Potassium (ug/dL)	6.4 ± 0.5	6.5 ± 0.2	7.3 ± 0.8	7.6 ± 0.9*	7.5 ± 2.8	6.5 ± 0.5	7 ± 0.5
Iron (umol/L)	47.4 ± 9.5	35 ± 4.2*	45.8 ± 8.6	40.8 ± 5.5	44 ± 11.5	43.2 ± 8.3	51.8 ± 7
Sodium (mmol/L)	136.8 ± 1.6	139.4 ± 1.2**	139.2 ± 1.3*	137.7 ± 0.8	135.9 ± 4.	138.8 ± 1*	137.4 ± 1.3

Results given as mean ± SD (* $P < 0.05$; ** $P < 0.001$ vs. control)

Ni FPs nickel fine particles, *Ni NPs*, nickel nanoparticles, *TP* total protein, *ALP* alkaline phosphatase, *AST* aspartate transaminase, *ALT* alanine aminotransferase, *Total B* total bilirubin, *Direct B* conjugated bilirubin, *BUN* blood urea nitrogen, *CK* creatine kinase, *CK-MB* creatine kinase isoenzymes, *HDL-C* high-density lipoproteincholesterol

Table 3 Hematological parameters of 35 SD rats after treatments with Ni NPs or FPs

Parameters	Control	Ni NPs (mg/kg)			Ni FPs (mg/kg)		
		5.6	12	25	5.6	12	25
WBC (10^9/L)	8 ± 2.8	9.9 ± 2.7	8.36 ± 4.2	5.84 ± 1.5	8.84 ± 2.3	9.1 ± 3.1	8.6 ± 1.6
NE%	12.1 ± 1.8	17.8 ± 7.8	10.62 ± 2.5*	11.3 ± 1.8	14.6 ± 8.3	8.5 ± 1.6	14.8 ± 8.5*
Ly%	83.1 ± 2.5	85.3 ± 3.3	85.8 ± 3	83.2 ± 4.5	88.9 ± 2.9*	88.2 ± 3.1*	86 ± 2.1
Mo%	4.3 ± 1.2	2.2 ± 0.8*	3.24 ± 1	4.4 ± 3.5	2.1 ± 0.9*	2.3 ± 1.2*	3 ± 0.5
Eo%	0.4 ± 0.3	0.3 ± 0.2	0.26 ± 0.3	0.27 ± 0.1	1.6 ± 3	1.1 ± 2.1	0.25 ± 0.2
RBC (10^{12}/L)	6.8 ± 0.3	6.8 ± 0.4	6.93 ± 0.5	6.7 ± 0.6	7 ± 0.4	6.9 ± 0.3	7.3 ± 0.5
HGB (g/L)	137.8 ± 3.4	136.2 ± 3.8	136.4 ± 9.2	132.8 ± 10.2	142 ± 7	137.8 ± 4.9	144.5 ± 6.9
MCHC (g/L)	338.6 ± 5.9	335.2 ± 4	332 ± 4.4	330.2 ± 2.7*	332.4 ± 2.5	333.2 ± 5.2	335.5 ± 7.5
PLT (10^9/L)	777.4 ± 361	822.6 ± 138	1153.8 ± 241.42	820.4 ± 169.7	940.4 ± 123.9	929.8 ± 206.6	889.8 ± 130.4

Results given as mean ± SD (* $P < 0.05$ vs. control)

Ni FPs nickel fine particles, *Ni NPs* nickel nanoparticles, *WBC* whole blood count, *NE%* neutrophil %, *Ly%* lymphocyte %, *Mo%* monocyte %, *Eo%* eosinophil %, *RBC* red blood cells, *HGB* hemoglobin, *MCHC* mean corpuscular hemoglobin concentration, *PLT* platelet
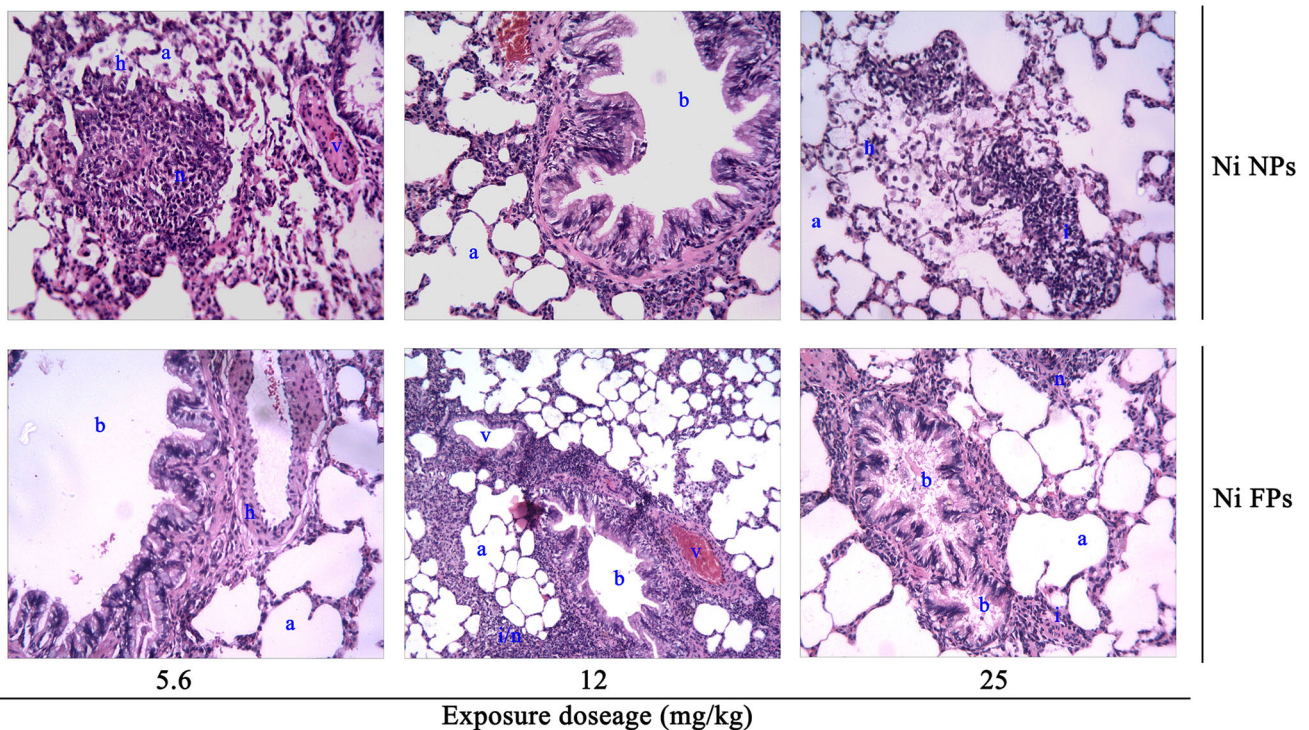

Fig. 6 Photomicrographs of lung histopathology. *Note* the images (magnification 20×) represent the histopathological observations in the lungs of the rats treated with different doses of Ni NPs or Ni FPs. The objectives used are as stated on the images (*a* alveolar spaces, *b* bronchioles, *h* histiocytes, *i* inflammatory cell infiltrates, *n* nodules, *v* veins). *Ni FPs* nickel fine particles, *Ni NPs* nickel nanoparticles

burning point (Zhang et al. 2003). However, these same properties of metallic nickel nanoparticles may present unique potential health impact. Furthermore, it is well known that the toxicity of particles to the lung in both occupational and environmental settings is not only related to exposure but also to the particle size (Zhao et al. 2009a). Accordingly, the aim of the present study is using both in vitro and in vivo experiments to compare the cyto- and genotoxicity induced by metallic Ni NPs and Ni FPs.
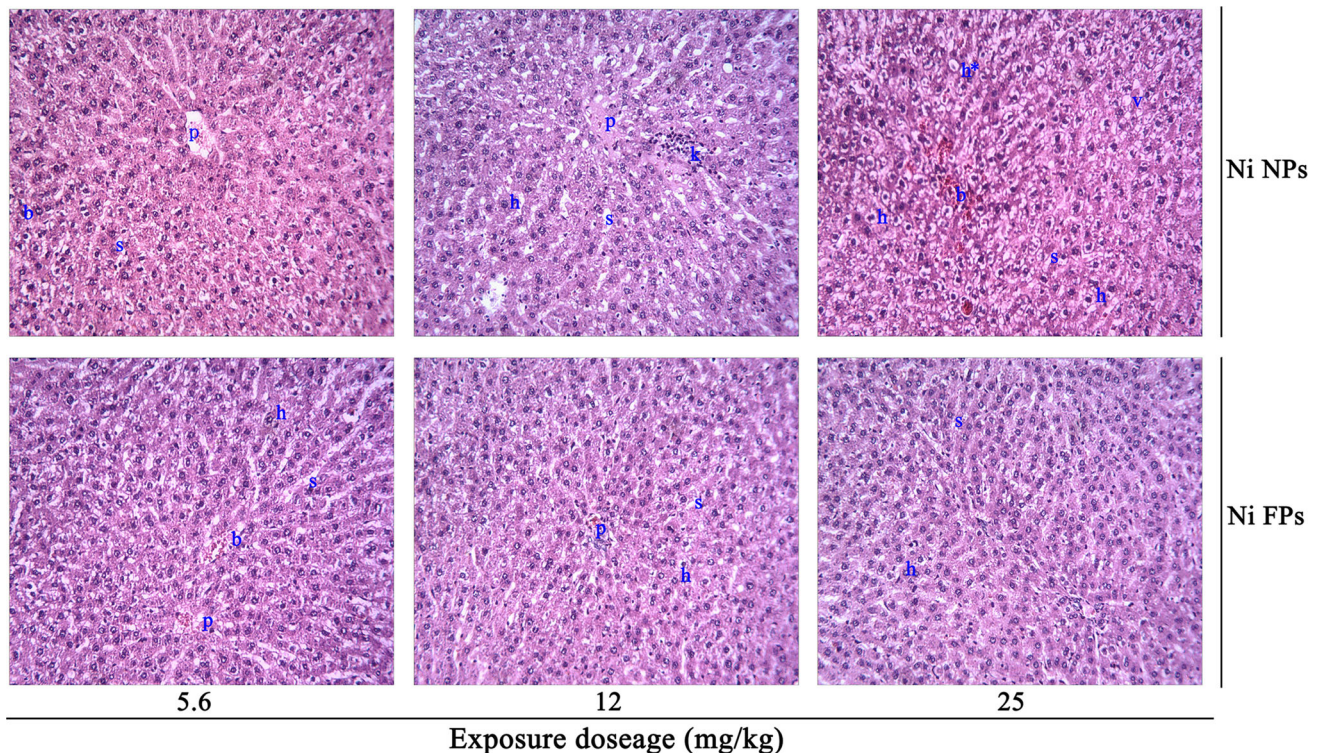
Fig. 7 Photomicrographs of liver histopathology. *Notes* the images (magnification 20×) represent the histopathological observations in the liver of the rats treated with different dose of Ni NPs or Ni FPs. The objectives used are as stated on the images (*p* liver portal, *h* liver hepatocytes, *s* sinus, *k* kuffer cells, *v* vacuoles, *h** enlarged hepatocytes). *Ni FPs* nickel fine particles, *Ni NPs* nickel nanoparticles

In vitro studies

Ni NPs decreased cell viability

Cellular stress can cause a depletion in ATP (Chantong et al. 2014). In this study, the cell titer Glo assay which measures the number of viable cells by detecting the amount of ATP present in the medium was used to evaluate the toxicity induced by the particles. The results showed that the number of viable cells decreased for both particle types as the dose increased. Under the same dose range, Ni NPs induced more A549 cell death than Ni FPs. Our findings were similar to that of Ahmed et al. who also observed dose dependent pattern of reduction in Human Breast Carcinoma (MCF-7) cells with increasing doses of Ni NPs. These suggest that Ni NPs may cause greater cellular stress than Ni FPs and these effects maybe increased in case of high exposure settings.

Ni NPs activate tumorigenic genes and causes DNA damage to a greater extent than Ni FPs

C-myc is a proto-oncogene, (Magaye et al. 2014; Tanaka et al. 2009) which usually involves in cell transformation, differentiation and cell-cycle progression and also has a central role in some forms of apoptosis (Shin et al. 2016). It is one of the most frequently affected genes in human cancers (Hoffman and Liebermann 2008; Richart et al. 2016). HO-1 as a stress-responsive protein is induced under conditions of different stress and has been implicated in cellular defense against oxidative stress (do Sameiro-Faria et al. 2014). Nrf2 is a master regulator of the antioxidant response and xenobiotic metabolism through the regulation of a wide range of antioxidant and Phase II detoxification genes (Bhakkiyalakshmi et al. 2016; Cao et al. 2016). All of these proteins play pivotal roles in the development and progression of tumors. The effect that NPs may exert on the DNA regulatory mechanisms which may translate into the production of tumors within the host is an area of great research and concern. Therefore, to determine the level of the tumorigenic gene activation by any given agent is of importance. Other researchers have observed that Ni nano compounds (Horie et al. 2011) and Ni FPs (Zhang et al. 2009) do induce increased expression of these (C-myc, HO-1 and Nrf2) proteins. The degradation of C-myc by Ni FP compounds ($NiSO_4$) has been mentioned, (Li et al. 2009a, b) indicating that $NiSO_4$ may promote cancer suppression in hypoxia states. However, it is yet to be shown if the same applies to Ni NPs.
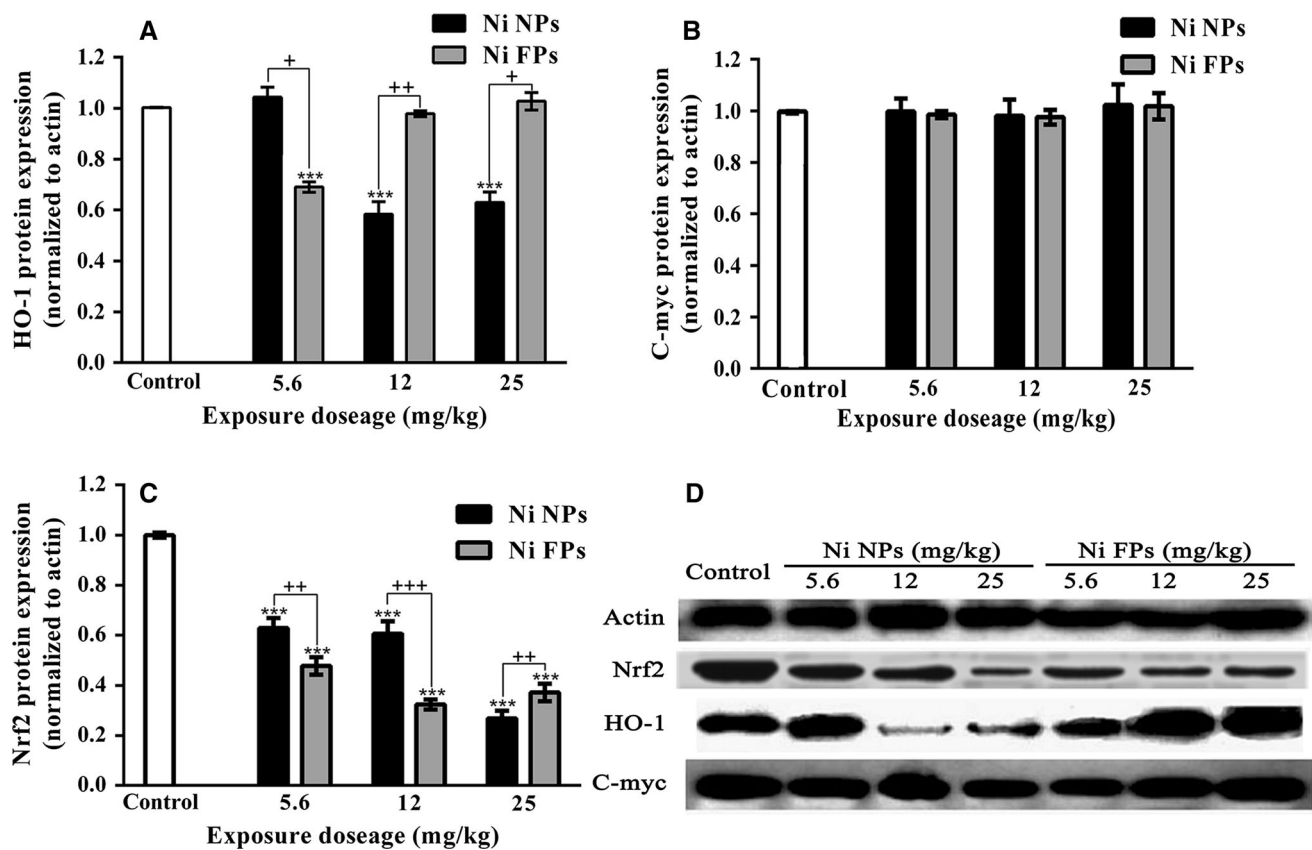
Fig. 8 HO-1, Nrf2 and C-myc protein expressions in the rat lung tissues. *Ni FPs* nickel fine particles, *Ni NPs* nickel nanoparticles

In this study, it was shown that Ni NPs and FPs may not elicit similar cellular responses in in vitro and in vivo models. Oberdoster (2010) has also mentioned that significant differences in responses can result when using different modes of administration, for example dosing respiratory epithelial cells in culture media and aerosol spray via an air–liquid interface model for in vivo study. In this study on A549 cells, the increased expression of HO-1 in both Ni NP and FP treated cells is an indication of the cells undergoing oxidative stress (Fig. 3). The expression of HO-1 has been shown to be a response to oxidative stress (Gao et al. 2016; Kooter et al. 2006). Overall, increased expression of HO-1 in NP treated cells was more prominent than in FP treated cells. Our results also showed a significant increase in the expression of C-myc protein in Ni NP treated cells. A study has shown the association of DNA damage with increased C-myc expression, in part through ROS generation (Kooter et al. 2006). These finding also suggests that Ni NPs may induce increased expression of the C-myc protein through ROS generation. The generation of ROS by Ni nanoparticles is supported by Ahamed et al. (2011) and Neubauer et al. (2015) who also noted that Ni NPs cause oxidative stress through a time, dose and size dependent manner respectively, by inducing

ROS production. However, we have also inferred in our previous study on JB6 cells treated with Ni NPs, that Ni NPs may cause genotoxic effects through increased HIF-1α expression leading to increased C-myc expression induced by hypoxic conditions (Magaye et al. 2014). We assume these differences to be due to type of cell used. However further studies that include the investigation of the expression of HIF-1α in A549 cells treated with Ni NPs are needed to clearly define the role of ROS and hypoxic conditions in the expression of C-myc and HO-1 since a study has shown increased *HO-1* gene expression in hypoxic conditions in conjunction with HIF-1α upregulation in cases of hypoxia-induced pulmonary hypertension in pulmonary arteries of rats (Li and Dai 2004). It can be assumed that Ni NPs may cause genotoxicity through more than 1 pathway. This implies that Ni NPs have the potential to cause oxidative stress and also to create a hypoxic environment. Other studies have shown that Ni NPs (100 nm) cause greater DNA damage (20–24 %), when compared to the known genotoxic compound titanium oxide in A549 cells (Park et al. 2007). We also observed similar percentage of DNA damage in this study (Fig. 5). Ni NPs caused about 15–20 % DNA damage and Ni FPs caused about 16–18 % damage in A549 cells. Significant

DNA damage was observed in cells treated with 10–25 $\mu g/cm^2$ Ni NPs and not in the 1–5 $\mu g/cm^2$. Whereas, in Ni FPs treated groups the DNA damage was only significant in the high dose group of 25 $\mu g/cm^2$. These damages were thought to be due to indirect interaction of Ni particles with cell DNA and epigenetic factors such as abnormal apoptosis, oxidative stress and persistent inflammatory reactions (Magaye and Zhao 2012; Magaye et al. 2012). Taking into consideration the amount of DNA damage caused by Ni NPs (Figs. 4, 5), even though there were no significant changes in the expression of Nrf2 in Ni nano and fine particle treated A549 cells, it can be inferred that Ni NPs may induce genotoxicity through increased expression of C-myc in the presence of ROS. C-myc expression is increased in a lot of tumors (Cui et al. 2015; Delgado et al. 2013).

In vivo studies

Ni NPs and FPs cause liver and kidney damage

The biochemical analysis for the SD rats treated with Ni NPs and FPs were also varied. However, the results showed that there was liver damage in both the NPs and FPs treated groups. The liver is one of the main organs involved in first pass metabolism (Kanazu et al. 2005). In Ni NPs treated groups the total bilirubin levels were significantly decreased, and this decrease was greatest at the high dose level. The direct bilirubin levels for the 12 and 25 mg/kg dose groups were also decreased significantly in a dose dependent manner. Even though low bilirubin levels may not be of concern, studies on patients with chronic kidney disease (CKD) on hemodialysis (do Sameiro-Faria et al. 2014; Sakoh et al. 2015) and coronary artery disease (CAD) (Tanaka et al. 2009; Zhu et al. 2016) have shown that low serum bilirubin levels leads to increased adverse effects. Bilirubin plays a protective role in reducing inflammatory responses and preventing the formation of plaques that can contribute to the pathogenesis of CKD and CAD possibly through it's role as an anti-oxidant and anti-inflammatory agent. Our results support Kang et al. (2011) research which showed that long term inhalation of nano Nickel hydroxide can cause cardiovascular toxicity by inducing oxidative stress and inflammation, which they concluded that it can lead to artherosclerosis in $ApoE^{-/-}$ mice. The reduced bilirubin in this study may imply changes in the lipid profile especially in conjuction with artherosclerotic changes that could increase the risk for CAD. This is supported by our findings which showed significant increase in serum levels of triglycerides in the 5.6 and 12 mg/kg Ni NP dose groups. Tryglycerides have been known to play a causal role in CAD (Do et al. 2013). Apart from this, no significant changes were observed in the serum cholestrol and HDL-C levels for all groups. Along with the increase in serum triglyceride levels in the 5.6 mg/kg Ni NP dose group, there was also a significant increase in serum CK levels. There was a general reduction in serum CK levels in all other dose groups which may be due to cachexia leading to wasting and general ill health as a result of the particles. This may also explain the significant decrease in the percentage of monocyte observed for the 5.6 mg/kg dose group of Ni NPs, and the 5.6 and 12 mg/kg dose groups of Ni FPs.

When more than 50 % of the total bilirubin is conjugated bilirubin, as is the case in the 25 mg/kg dose group, hepatocelluar injury can be suggested (Abboud and Kaplowitz 2007). In the 25 mg/kg Ni FP dose group the direct bilirubin was greatly reduced. This is also supported by the findings in the liver organ to body weight coefficients. Histopathological evidence showed that liver pathology was most prominent in the 25 mg/kg Ni FPs treated dose group (Fig. 7). The liver in this group showed extensive liver congestion. In the 12 mg/kg dose group treated with Ni NPs, there was an increase in the presence of kupffer cells (Fig. 7), while, in the 25 mg/kg dose group the size of the hepatocytes were increased and there was hemorrhage shown by the presence of aggregates of blood cells in the sinusoids. Similar liver injuries were noted in rats (Poland et al. 2012). Apart from lymphadenosis or enlargement of the lymph nodes in the 12 and 25 mg/kg dose groups treated with Ni NPs, the tissues from all other organs showed indistinguishable pathological changes.

Apart from the bilirubin components, other liver function tests such the total protein (TP) level was significantly increased in the 5.6 mg/kg Ni FP dose group. This may be caused by dehydration, which could also explain the significant increase in albumin levels in the 5.6 and 12 mg/kg dose groups. Even though, decreases in the ALT and AST levels were noticed, these were not statistically significant.

The renal profile showed that the blood urea nitrogen (BUN) level of 12 and 25 mg/kg dose groups treated with Ni FPs was reduced. However, all other dose groups showed no significant changes. Low BUN levels are associated with liver disease or malnutrition. The electrolytes, sodium (Na) and potassium (K) were increased in the 5 and 12 mg/kg (Ni NPs) and the 12 mg/kg (Ni FPs) treated dose groups. In normal settings, when Na rises, K decreases, however this may not be the case in disorders that decrease kidney function, such as chronic kidney disease. The level of iron (Fe) was reduced in the 5.6 mg/kg Ni NP dose group. A decrease in serum iron levels is a sign of anemia. However, the RBC and Hgb levels in all dose groups did not show any significant changes.

These results show that there was acute liver and kidney toxicity, and also shows the potential of Ni NP and FP to be

contributors to adverse effects in the prognosis of CKD and CAD.

Ni NPs and FPs caused lung cyto and genotoxicity

Histopathological examination of the lung tissues showed wide spread pathology in the lungs of all doses treated with either Ni NPs or FPs. The most prominent feature in all dose groups were the inflammatory cell infiltrates consisting of lymphocytes, neutrophils and macrophages. The aggregates of these infiltrates are interstitial and predominantly in a peri-bronchial location but they extend to the alveolar walls (Fig. 6). Histiocytes were scattered in all dose groups treated with Ni NPs. These features indicate the presence of inflammation and inflammatory hyperplasia. The hematological analysis showed that the percentage of neutrophils was decreased in the 12 mg/kg dose group (Ni NPs) and increased in the 25 mg/kg dose group (Ni FPs). The decrease in neutrophils is often due to enlargement of the spleen (lymphadenosis) which was in our study. The percentage of lymphocytes, were also increased in the 5.6 and 12 mg/kg dose groups of Ni FPs. Since the expression of HO-1 is cytoprotective, our study showed that the expression of HO-1 in the 12 and 25 mg/kg dose groups treated with Ni NP (Fig. 8a) was significantly reduced, which may lead to cyto and genotoxic effects on the lung as supported the histopathological findings. This reduction is also corroborated by the significant decrease in serum bilirubin in these dose groups, since HO-1 plays a key role in the pathway of heme degradation leading to the reduction of biliverdin to bilirubin. However, no significant differences in HO-1 protein expression were observed in the other dose groups treated with either Ni NPs or FPs. The decrease in HO-1 expression may also suggest decreased lung function due to lung burden overload in these dose groups. No changes were observed in the expression of C-myc in all dose groups treated with Ni NPs or FPs (Fig. 8b).

Conclusion

Overall, our study has shown that Ni NPs had higher cytotoxic and genotoxic effects than Ni FPs in in vitro as well as in in vivo studies under the same treatment dose. We have also shown that differences in modes of administration can lead to varied responses and effects on the biological systems. Furthermore, Ni NPs may exert cyto- and genotoxic damages through more than one pathway depending on the type of system, either through oxidative stress or hypoxia. Even though both Ni NPs and Ni FPs caused decreased cell viability in A549 cells in a dose dependent manner, Ni NPs had greater toxicity and caused

dose dependent DNA damage. While, Ni FPs induced DNA damage was only significant at the high dose.

Both Ni NPs and FPs caused differing degrees of acute toxicity, especially in the liver and lungs of SD rats. Apart from causing acute liver and kidney toxicity, the study also shows the potential for Ni NPs and FPs to be contributors to adverse effects in the prognosis of CKD and CAD. The level of cyto and genotoxic damage in the lungs by Ni NPs was most prominent with hyperplastic changes and decreased expression of HO-1 protein.

In conclusion, Ni NPs and FPs cause acute cytoxic and genotoxic effects. The in vitro results show that Ni NPs cause greater cyto- and genotoxicity, while the in vivo results show similar effects for both particle types and it also showed the potential effects metallic based nanoparticles can have on the prognosis of those organs with underlying diseases. The molecular mechanisms leading to these changes maybe varied in different systems. Thus, further studies to clarify the role of Ni NPs in inducing oxidative stress and hypoxia as well as the details of the molecular mechanisms of Ni NPs carcinogenicity are needed.

Authors' contributions J.Z. led all participators to design this study, was responsible for coordinating the study and drafted the manuscript. R.M., Y.W. and B.Z. conducted the animal experiments. Y.G., H.S. and Q.Z. conducted the in vitro experiments and processed the toxicological data. G.M., X.Y., H.S. and J.X. performed the data collection, interpretation and statistical analysis. R.M. and Y.G. contributed to the preparation of the manuscript. All authors read and approved the final manuscript.

References

Abboud G, Kaplowitz N (2007) Drug-induced liver injury. Drug Saf 30:277–294

Ada K et al (2010) Cytotoxicity and apoptotic effects of nickel oxide nanoparticles in cultured HeLa cells. Folia Histochem Cytobiol 48:524–529

Ahamed M (2011) Toxic response of nickel nanoparticles in human lung epithelial A549 cells. Toxicol In Vitro 25:930–936

Ahamed M, Alhadlaq HA (2014) Nickel nanoparticle-induced dose-dependent cyto-genotoxicity in human breast carcinoma MCF-7 cells. Onco Targets Ther 7:269–280

Ahamed M et al (2011) Oxidative stress mediated apoptosis induced by nickel ferrite nanoparticles in cultured A549 cells. Toxicology 283:101–108

Ahmad J et al (2016) Differential cytotoxicity of copper ferrite nanoparticles in different human cells. J Appl Toxicol. doi:10.1002/jat.3299

Alarifi S, Ali D, Alakhtani S, Al Suhaibani ES, Al-Qahtani AA (2014) Reactive oxygen species-mediated DNA damage and apoptosis in human skin epidermal cells after exposure to nickel nanoparticles. Biol Trace Elem Res 157:84–93

Baek YW, An YJ (2011) Microbial toxicity of metal oxide nanoparticles (CuO, NiO, ZnO, and Sb_2O_3) to Escherichia coli, Bacillus subtilis, and Streptococcus aureus. Sci Total Environ 409:1603–1608

Bhakkiyalakshmi E, Sireesh D, Sakthivadivel M, Sivasubramanian S, Gunasekaran P, Ramkumar KM (2016) Anti-hyperlipidemic and anti-peroxidative role of pterostilbene via Nrf2 signaling in experimental diabetes. Eur J Pharmacol. doi:10.1016/j.ejphar.2016.02.054

Cao LJ et al (2016) The protective effects of isoliquiritigenin and glycyrrhetinic acid against triptolide-induced oxidative stress in HepG2 cells involve Nrf2 activation. Evid Based Complement Altern Med. doi:10.1155/2016/8912184

Chantong B, Kratschmar DV, Lister A, Odermatt A (2014) Inhibition of metabotropic glutamate receptor 5 induces cellular stress through pertussis toxin-sensitive Gi-proteins in murine BV-2 microglia cells. J Neuroinflamm 11:190

Cui J et al (2015) c-Myc-activated long non-coding RNA H19 downregulates miR-107 and promotes cell cycle progression of non-small cell lung cancer. Int J Clin Exp Pathol 8:12400–12409

Das KK, Buchner V (2007) Effect of nickel exposure on peripheral tissues: role of oxidative stress in toxicity and possible protection by ascorbic acid. Rev Environ Health 22:157–173

Delgado MD, Albajar M, Gomez-Casares MT, Batlle A, Leon J (2013) MYC oncogene in myeloid neoplasias. Clin Transl Oncol 15:87–94

do Sameiro-Faria M et al (2014) Potential cardiovascular risk protection of bilirubin in end-stage renal disease patients under hemodialysis. Biomed Res Int. doi:10.1155/2014/175286

Do R et al (2013) Common variants associated with plasma triglycerides and risk for coronary artery disease. Nat Genet 45:1345–1352

Dorighello GG, Paim BA, Kiihl SF, Ferreira MS, Catharino RR, Vercesi AE, Oliveira HC (2016) Correlation between mitochondrial reactive oxygen and severity of atherosclerosis. Oxid Med Cell Longev. doi:10.1155/2016/7843685

Elbastawisy YM, Almasry SM (2014) Histomorphological evaluation of maternal and neonatal distal airspaces after maternal intake of nanoparticulate titanium dioxide: an experimental study in Wistar rats. J Mol Histol 45:91–102

Fahmy B, Cormier SA (2009) Copper oxide nanoparticles induce oxidative stress and cytotoxicity in airway epithelial cells. Toxicol In Vitro 23:1365–1371

Gao Z et al (2016) Targeting HO-1 by epigallocatechin-3-gallate reduces contrast-induced renal injury via anti-oxidative stress and anti-inflammation pathways. PLoS ONE. doi:10.1371/journal.pone.0149032

Gillespie PA et al (2010) Pulmonary response after exposure to inhaled nickel hydroxide nanoparticles: short and long-term studies in mice. Nanotoxicology 4:106–119

Hansen T et al (2006) Biological tolerance of different materials in bulk and nanoparticulate form in a rat model: sarcoma development by nanoparticles. J R Soc Interface 3:767–775

Hoffman B, Liebermann DA (2008) Apoptotic signaling by c-MYC. Oncogene 27:6462–6472

Horie M et al (2011) Evaluation of acute oxidative stress induced by NiO nanoparticles in vivo and in vitro. J Occup Health 53:64–74

Huk A et al (2015) Impact of nanosilver on various DNA lesions and HPRT gene mutations—effects of charge and surface coating. Part Fibre Toxicol. doi:10.1186/s12989-015-0100-x

Kanazu T, Okamura N, Yamaguchi Y, Baba T, Koike M (2005) Assessment of the hepatic and intestinal first-pass metabolism of midazolam in a CYP3A drug-drug interaction model rats. Xenobiotica. doi:10.1080/00498250500093786

Kang GS, Gillespie PA, Gunnison A, Moreira AL, Tchou-Wong KM, Chen LC (2011) Long-term inhalation exposure to nickel nanoparticles exacerbated atherosclerosis in a susceptible mouse model. Environ Health Perspect 119:176–181

Ke Q, Li Q, Ellen TP, Sun H, Costa M (2008) Nickel compounds induce phosphorylation of histone H3 at serine 10 by activating JNK-MAPK pathway. Carcinogenesis 29:1276–1281

Kooter IM, Boere AJ, Fokkens PH, Leseman DL, Dormans JA, Cassee FR (2006) Response of spontaneously hypertensive rats to inhalation of fine and ultrafine particles from traffic: experimental controlled study. Part Fibre Toxicol. doi:10.1186/1743-8977-3-7

Li QF, Dai AG (2004) Hypoxia inducible factor-1 alpha correlates the expression of heme oxygenase 1 gene in pulmonary arteries of rat with hypoxia-induced pulmonary hypertension. Acta Biochim Biophys Sin (Shanghai) 36:133–140

Li Q, Kluz T, Sun H, Costa M (2009a) Mechanisms of c-myc degradation by nickel compounds and hypoxia. PLoS ONE. doi:10.1371/journal.pone.0008531

Li Q, Suen TC, Sun H, Arita A, Costa M (2009b) Nickel compounds induce apoptosis in human bronchial epithelial Beas-2B cells by activation of c-Myc through ERK pathway. Toxicol Appl Pharmacol 235:191–198

Liu GY, Sun YZ, Zhou N, Du XM, Yang J, Guo SJ (2016) 3,3′-OH curcumin causes apoptosis in HepG2 cells through ROS-mediated pathway. Eur J Med Chem 112:157–163

Lu H, Shi X, Costa M, Huang C (2005) Carcinogenic effect of nickel compounds. Mol Cell Biochem 279:45–67. doi:10.1007/s11010-005-8215-2

Magaye R, Zhao J (2012) Recent progress in studies of metallic nickel and nickel-based nanoparticles' genotoxicity and carcinogenicity. Environ Toxicol Pharmacol 34:644–650

Magaye R, Zhao J, Bowman L, Ding M (2012) Genotoxicity and carcinogenicity of cobalt-, nickel- and copper-based nanoparticles. Exp Ther Med 4:551–561

Magaye RR et al (2014) Acute toxicity of nickel nanoparticles in rats after intravenous injection. Int J Nanomed 9:1393–1402

Morimoto Y, Kobayashi N, Shinohara N, Myojo T, Tanaka I, Nakanishi J (2010) Hazard assessments of manufactured nanomaterials. J Occup Health 52:325–334

Mueller NC et al (2012) Nanofiltration and nanostructured membranes–should they be considered nanotechnology or not? J Hazard Mater. doi:10.1016/j.jhazmat.2011.10.096

Neubauer N, Palomaeki J, Karisola P, Alenius H, Kasper G (2015) Size-dependent ROS production by palladium and nickel nanoparticles in cellular and acellular environments—an indication for the catalytic nature of their interactions. Nanotoxicology 9:1059–1066

Oberdorster G (2010) Safety assessment for nanotechnology and nanomedicine: concepts of nanotoxicology. Intern Med 267:89–105

Ogami A, Morimoto Y, Murakami M, Myojo T, Oyabu T, Tanak I (2009) Biological effects of nano-nickel in rat lungs after administration by inhalation and by intratracheal instillation. J Phys Conf Ser. doi:10.1088/1742-6596/151/1/0120325

Oyabu T, Ogami A, Morimoto Y, Shimada M, Lenggoro W, Okuyama K, Tanaka I (2007) Biopersistence of inhaled nickel oxide nanoparticles in rat lung. Inhal Toxicol. doi:10.1080/08958370701492995

Park S et al (2007) Cellular toxicity of various inhalable metal nanoparticles on human alveolar epithelial cells. Inhal Toxicol. doi:10.1080/08958370701493282

Poland CA et al (2012) Length-dependent pathogenic effects of nickel nanowires in the lungs and the peritoneal cavity. Nanotoxicology 6:899–911

Pujalte I, Passagne I, Brouillaud B, Treguer M, Durand E, Ohayon-Courtes C, L'Azou B (2011) Cytotoxicity and oxidative stress induced by different metallic nanoparticles on human kidney cells. Part Fibre Toxicol. doi:10.1186/1743-8977-8-10

Richart L, Carrillo-de Santa Pau E, Rio-Machin A, de Andres MP, Cigudosa JC, Lobo VJ, Real FX (2016) BPTF is required for c-MYC transcriptional activity and in vivo tumorigenesis. Nat Commun. doi:10.1038/ncomms10153

Ryter SW, Kim HP, Hoetzel A, Park JW, Nakahira K, Wang X, Choi AM (2007) Mechanisms of cell death in oxidative stress. Antioxid Redox Signal 9:49–89

Sakoh T et al (2015) Association of serum total bilirubin with renal outcome in Japanese patients with stages 3–5 chronic kidney disease. Metabolism 64:1096–1102

Saradhi M, Krishna B, Mukhopadhyay G, Tyagi RK (2005) Purification of full-length human pregnane and xenobiotic receptor: polyclonal antibody preparation for immunological characterization. Cell Res 15:785–795

Shi H, Magaye R, Castranova V, Zhao J (2013) Titanium dioxide nanoparticles: a review of current toxicological data. Part Fibre Toxicol. doi:10.1186/1743-8977-10-15

Shin JM, Jeong YJ, Cho HJ, Magae J, Bae YS, Chang YC (2016) Suppression of c-Myc induces apoptosis via an AMPK/mTOR-dependent pathway by 4-O-methyl-ascochlorin in leukemia cells. Apoptosis. doi:10.1007/s10495-016-1228-3

Sivulka DJ (2005) Assessment of respiratory carcinogenicity associated with exposure to metallic nickel: a review. Regul Toxicol Pharmacol 43:117–133

Tanaka M et al (2009) Low serum bilirubin concentration is associated with coronary artery calcification (CAC). Atherosclerosis 206:287–291

Yang H, Liu C, Yang D, Zhang H, Xi Z (2009) Comparative study of cytotoxicity, oxidative stress and genotoxicity induced by four typical nanomaterials: the role of particle size, shape and composition. J Appl Toxicol 29:69–78

Yang L, Meng H, Yang M (2016) Autophagy protects osteoblasts from AGEs induced apoptosis through intracellular ROS. J Mol Endocrinol. doi:10.1530/jme-15-0267

Zaman S, Wang R, Gandhi V (2015) Targeting executioner procaspase-3 with the procaspase-activating compound B-PAC-1 induces apoptosis in multiple myeloma cells. Exp Hematol 43(951–962):e3

Zhang Q, Kusaka Y, Zhu X, Sato K, Mo Y, Kluz T, Donaldson K (2003) Comparative toxicity of standard nickel and ultrafine nickel in lung after intratracheal instillation. J Occup Health 45:23–30

Zhang D, Shen J, Wang C, Zhang X, Chen J (2009) GSH-dependent iNOS and HO-1 mediated apoptosis of human Jurkat cells induced by nickel(II). Environ Toxicol 24:404–414

Zhao J, Bowman L, Zhang X, Shi X, Jiang B, Castranova V, Ding M (2009a) Metallic nickel nano- and fine particles induce JB6 cell apoptosis through a caspase-8/AIF mediated cytochrome c-independent pathway. J Nanobiotechnol 7:1477–3155

Zhao J, Bowman L, Zhang X, Shi X, Jiang B, Castranova V, Ding M (2009b) Metallic nickel nano- and fine particles induce JB6 cell apoptosis through a caspase-8/AIF mediated cytochrome c-independent pathway. J Nanobiotechnol. doi:10.1186/1477-3155-7-2

Zhu KF, Wang YM, Wang YQ, Wang NF (2016) The relationship between serum levels of total bilirubin and coronary plaque vulnerability. Coron Artery Dis 27:52–58

Zou P et al (2016) EF24 induces ROS-mediated apoptosis via targeting thioredoxin reductase 1 in gastric cancer cells. Oncotarget. doi:10.18632/oncotarget.7633